lateral shear causing seismicity related to both strike-slip and normal faulting. Between 1994 and 1998, the area experienced episodic swarms of enhanced seismicity attributed to magma moving within the system. Activity culminated in a magnitude 5.1 earthquake on June 4, 1998, and a magnitude 5 earthquake on November 13, 1998. Geodetic measurements using GPS, levelling and InSAR detected uplift and expansion of the volcanic edifice above a point source of pressure beneath the Hrómundartindur volcanic system. Magma accumulation elevated the volcanic edifice 2 cm/year and is believed to have triggered motion along strike-slip faults that were near to failure due to tectonic stresses. A number of faults in the area generated small-scale surface breaks. Geographic information system has been used to integrate aerial photographs, field data and geophysical data to determine how the crust breaks in response to deformation along this plate boundary, and to see how much of the recent activity focussed on pre-existing weaknesses in the crust. Our data indicates that all surface rupture has occurred along or adjacent to old faults, several of which were previously unmapped. The most prominent surface breaks occurred along NE- and NNE-trending faults adjacent to the epicenter of the June 4 earthquake. Maximum opening observed along a single fault segment was 1.2 m. Styles of rupture include fresh rockfall into pre-existing fissures and along old scarps, subsidence along and possible widening of old fissures, tears in turf and gashes in soil, shattering of lava blocks and loosening of push-up structures related to strike-slip faulting (Figure 30). Although all geophysical data agree that rupture occurred along a shallow, right-lateral strike-slip fault, no clear evidence of lateral offset was observed at the surface. Foreshocks and aftershocks from the November 13 earthquake define a broad E-W zone that intersects the southern end of the June 4 fault. The only surface rupture observed in this zone was found at that intersection.

In addition to fault mapping in the Hengill area, then Páll Einarsson at UICE.SI worked as a subcontractor on preparing a digitized fault map of the South Iceland seismic zone, as described in the PRENLAB-2 first annual report. That work is still in progress.

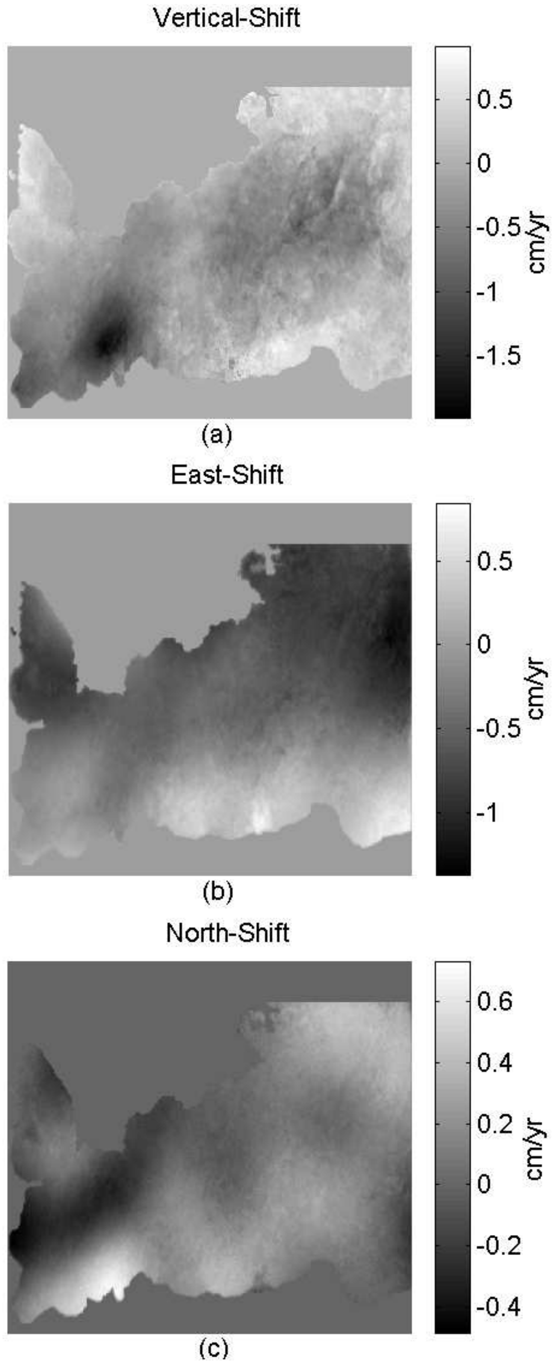

Figure 29. *Estimated one-year average motion field maps at the Reykjanes peninsula. (a), (b) and (c): Average vertical, east and north motion maps, respectively, inferred by the 1992-1993, 1992-1995, 1992-1996 and 1993-1995 InSAR data, and the 1993-1998 GPS data (Guðmundsson et al. 2000).*

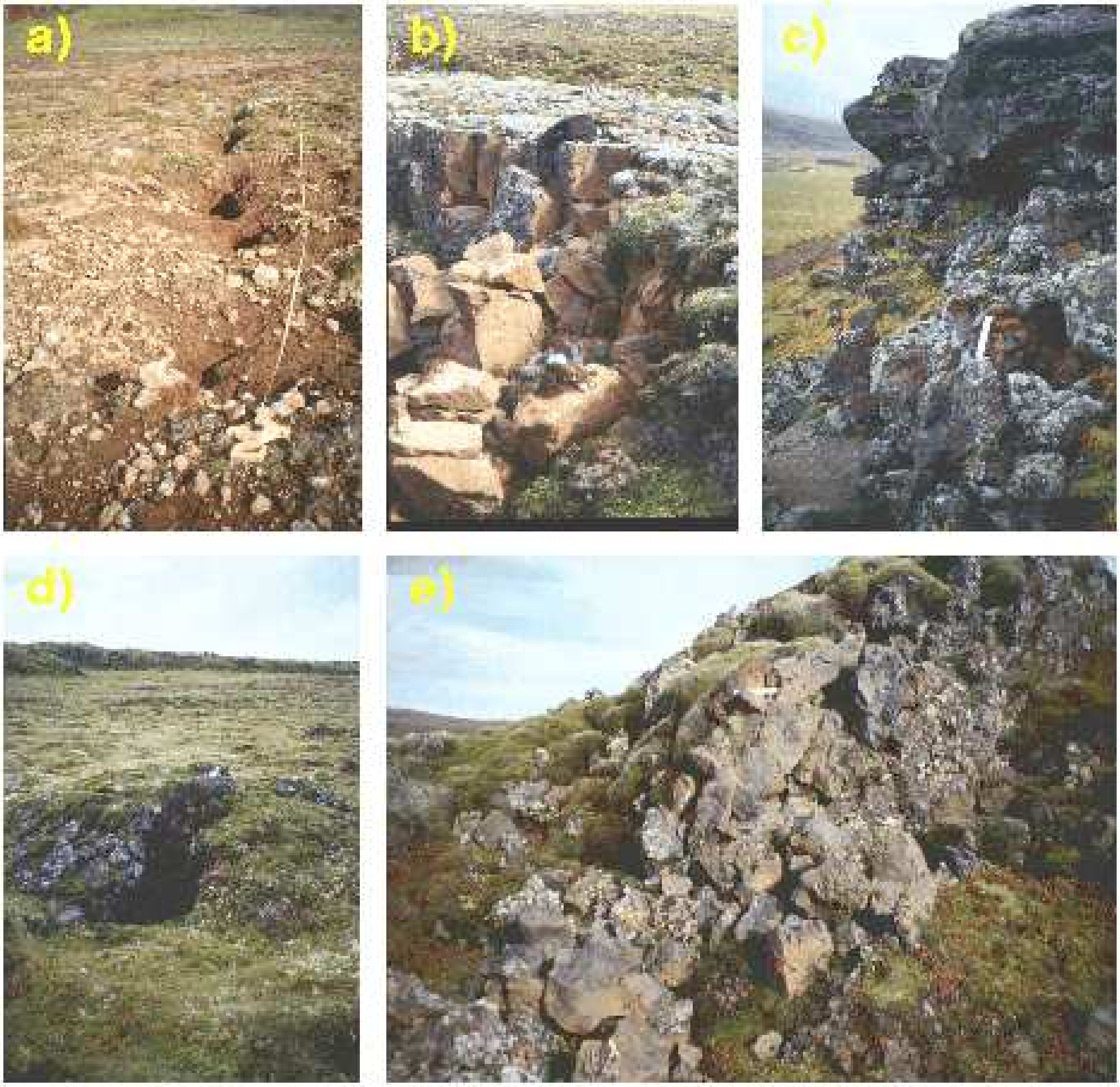

Figure 30. *Different styles of surface rupture observed in the Hengill area in response to uplift, and the June 4, 1998, M=5.1 earthquake. a) Gashes in soil: Ellipital segments up to 1.5 m wide, 2 m long, more than 1 m deep, en-echelon and along-strike arrangement. b) Rock fall along old fissures: Unweathered surfaces of broken rock, free of vegetation, plant roots freshly exposed. c) Rock fall along old fault scarps: Large fallen blocks, exposing freshly torn plant roots and soil, large rocks dislodged from slope leaving gaps between rocks and soil. d) Loosened push-up structures: Piles of rock with gaps of up to several centimeters between rock and soil; individual rocks may show evidence of rotation. e) Shattered aa lava: Broken blocks up to 1 m in diameter, aligned along strike and at flow margins near the June earthquake epicenter (Clifton 2000).*

3.5.3 References

Clifton, A. 2000. Surface deformation related to volcanic uplift and seismicity in SW-Iceland. Poster presented at the Nordvulk-Ridge summer school, Iceland, August 20-30, 2000.

Clifton, A. & F. Sigmundsson 2000. Faulting and deformation resulting from magma accumulation at the Hengill triple junction, SW-Iceland. In: Abstracts from the AGU fall meeting, San Francisco, California, USA, December 15-19, 2000.

Feigl, K.L., J. Gasperi, F. Sigmundsson & A. Rigo 2000. Crustal deformation near Hengill volcano, Iceland, 1993-1998: coupling between magmatic activity and faulting inferred from elastic modeling of satellite radar interferograms, *J. Geophys. Res.* 105, 25655-25670.

Guðmundsson, S., F. Sigmundsson & J.M. Carstensen 2000. Three-dimensional surface motion maps estimated from combined InSAR and GPS data. *J. Geophys. Res.*, submitted.

Hreinsdóttir, S., P. Einarsson, & F. Sigmundsson 2000. Crustal deformation at the oblique spreading Reykjanes peninsula, SW-Iceland: GPS measurements from 1993 to 1998. *J. Geophys. Res.*, submitted.

Miller, A.D., B.R. Julian & G.R. Foulger 1998. Three dimensional seismic structure and moment tensors of non-double-couple earthquakes at Hengill-Grensdalur volcanic complex, Iceland. *Geophys. J. Int.* 133, 309-325.

Rögnvaldsson, S.Th., G.B. Guðmundsson, K. Ágústsson, S.S. Jakobsdóttir, R. Slunga & R. Stefánsson 1998a. Overview of the 1993-1996 seismicity near Hengill. *Rit Veðurstofu Íslands* VÍ-R98006-JA05. Research report, Icelandic Meterological Office, Reykjavík, 16 pp.

Rögnvaldsson, S. Th., Þ. Árnadóttir, K. Ágústsson, Þ. Skaftadóttir, G.B. Guðmundsson, G. Björnsson, K.S. Vogfjörð, R. Stefánsson, R. Böðvarsson, R. Slunga, S.S. Jakobsdóttir, B.S. Þorbjarnardóttir, P. Erlendsson, B.H. Bergsson, S. Ragnarsson, P. Halldórsson, B. Þorkelsson & M. Ásgeirsdóttir 1998b. Skjálftahrina í Ölfusi í nóvember 1998. *Greinargerð Veðurstofu Íslands* VÍ-G98046-JA09. Report, Icelandic Meteorological Office, Reykjavík, 19 pp. In Icelandic.

Vadon, H., & F. Sigmundsson 1997. Crustal deformation from 1992 to 1995 at the mid-Atlantic ridge, Southwest Iceland, mapped by satellite radar interferometry. *Science* 257, 194-197.

3.6 Subproject 6: Effects of stress fields and crustal fluids on the development and sealing of seismogenic faults

Contractor:

Françoise Bergerat
Département de Géotectonique, Boite 129
Université Pierre et Marie Curie
4, place Jussieu
FR-75252 Paris Cedex 05
France
Tel: 33-1-4427-3443
Fax: 33-1-4427-5085
E-mail: bergerat@lgs.jussieu.fr

Subcontractor:

Jacques Angelier
Département de Géotectonique, Boite 129
Université Pierre et Marie Curie
4, place Jussieu
FR-75252 Paris Cedex 05
France
Tel: 33-1-4427-5857
Fax: 33-1-4427-5085
E-mail: jacques.angelier@lgs.jussieu.fr

Subcontractor:

Ágúst Guðmundsson
Geological Institute
University of Bergen
Allégaten 41
N-5007 Bergen
Norway
Tel: 47-5558-3503
Fax: 47-5558-9416
E-mail: agust.gudmundsson@geol.uib.no

Subcontractor:

Thierry Villemin
Laboratoire de Geodynamique des Chaines Alpines
Université de Savoie
Batiment Belledonne
Domaine Universitaire
73376 Le Bourget du Lac Cedex
France
Tel: 33-4-7975-8735
Fax: 33-4-7975-8777

E-mail: Thierry.Villemin@univ-savoie.fr

Subcontractor:

Philip Meredith
Department of Geological Sciences
University College London
Gower Street
London WC1E 6BT
United Kingdom
Tel: 44-171-380-7822
Fax: 44-171-387-1612
E-mail: p.meredith@ucl.ac.uk

3.6.1 Task 1: Determination of the paleostress fields associated with the test areas from fault-slip data

3.6.1.1 Task 1.1: The South Iceland seismic zone (SISZ)

We carried out a structural study in this area, including analysis of aerial photographs, local observation of major faults and collection of minor fault slip data in outcrops, as well as an analysis of the focal mechanisms of earthquakes (Bergerat et al. 1998; Bergerat et al. 1999; Bergerat and Angelier 2000). At the regional scale, the main fault trends are approximately NNE-SSW and NE-SW. ENE-WSW, NW-SE and WNW-ESE trending faults are also detected in aerial photographs and in the field. All these faults are normal or strike-slip in character. Some of the historical major earthquake fractures are observed in the post-glacial lava flows in the SISZ: most are right-lateral and trend roughly N-S. We analyzed more than 700 minor faults at 25 sites. Most sites are located in rocks of Upper Pliocene-Pleistocene age. Inversion of fault-slip datasets enabled us to reconstruct local paleostress tensors, hence to define the major tectonic regimes which have prevailed in the SISZ. Two main groups of faulting mechanisms reveal two distinct stress regimes, with perpendicular directions of extension, NW-SE (primary) and NE-SW (secondary). Both groups, however, display inhomogeneous datasets, related to extensional and to strike-slip faulting. The primary stress regime is in agreement with both the general behaviour of the SISZ as a left-lateral transform zone and the opening of the rift segments. The secondary stress regime, incompatible with the primary stress regime, is interpreted in terms of stress permutations. A population of 231 double-couple focal mechanisms ($M>1$ and depth>2 km) was also analyzed in terms of stress states. The results show great similarity in terms of stress directions. Figure 31 gives an example of a characteristic fault-slip data site and a comparison with focal mechanisms of earthquakes.

The present-day stress field mainly inferred from analyses of earthquake focal mechanisms is consistent with the present behaviour of the SISZ as a left-lateral transform zone. However, the proportion of strike-slip faulting within the present-day seismic activity (71%) is significantly higher than that revealed by the geological observation of Quaternary faults (50%). This contrast is interpreted in terms of development and evolution of the transform fault zone. Figure 32 schematically presents a comparison between the paleostress results obtained from faulting analysis and the present day activity based on focal mechanisms of

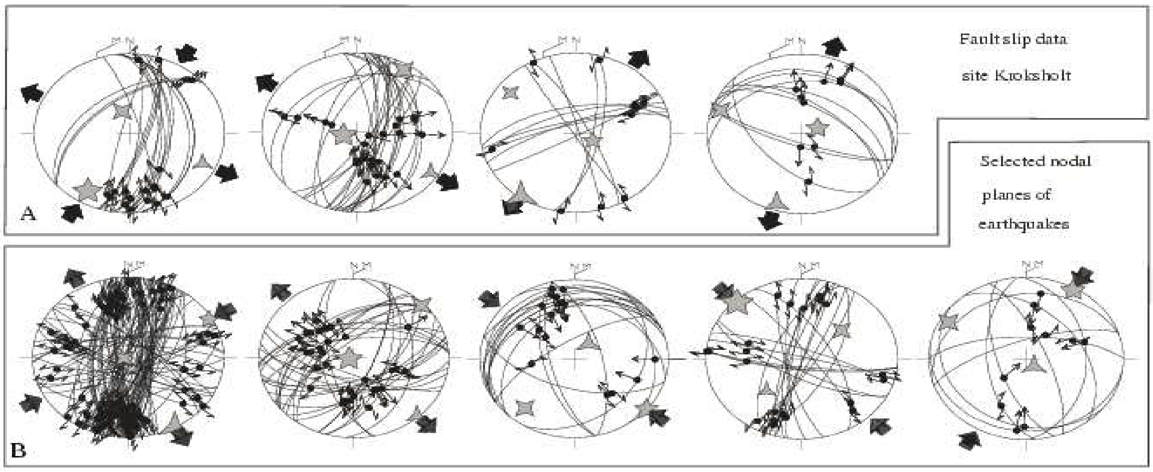

Figure 31. *Comparison between the main stress regimes as indicated by fault–slip datasets and focal mechanisms of earthquakes in the SISZ, based on two case examples (after Bergerat and Angelier 2000). (A) Striated faults at site Króksholt. (B) Selected nodal planes and slip vectors of earthquakes throughout the SISZ for the years 1991-1994 and 1996, at crustal depths larger than 2 km, with magnitudes larger than 1.*

earthquakes analysis. Stress permutations between different regimes are shown as couples of open arrows. The paleostress fields identified in the Upper Pliocene-Pleistocene formations of the SISZ reflect both the previous behaviour of the area, when it was located inside the rift zone, and its present behaviour as a transform zone, thus illustrating the local evolution from rifting to transform motion.

3.6.1.2 Task 1.2: The Tjörnes fracture zone (TFZ)

The inversion of about 1000 fault-slip data collected in 20 sites in the Flateyjarskagi peninsula allows reconstruction of eight normal and strike-slip regimes (Angelier et al. 2000b; Bergerat et al. 2000) related to the general behaviour of the Húsavík-Flatey fault (HFF), a major structure of the Tjörnes fracture zone connecting the Kolbeinsey ridge and the North Icelandic rift. The two most important regimes (E-W and NE-SW extensions), consistent with the right-lateral motion along the Húsavík-Flatey fault, constitute the main tectonic group. The two others (NW-SE and N-S extensions), forming the subordinate tectonic group, are incompatible and result from drastic stress permutations (as a probable result of stress drop, elastic rebound and dyke injection). Figure 33 summarizes the local paleostress determinations made in Flateyjarskagi.

The relationships between these stress regimes imply not only σ_1/σ_2 and σ_2/σ_3 stress permutations, but also σ_1/σ_3 reversals. An important factor controlling the transform mechanism is the variation of coupling along the HFF. The obliquity between the direction of transform motion and the trend of extension for the two main regimes may vary between 25° and 85°, reflecting repeated changes of the coefficient of friction along the HFF (Figure

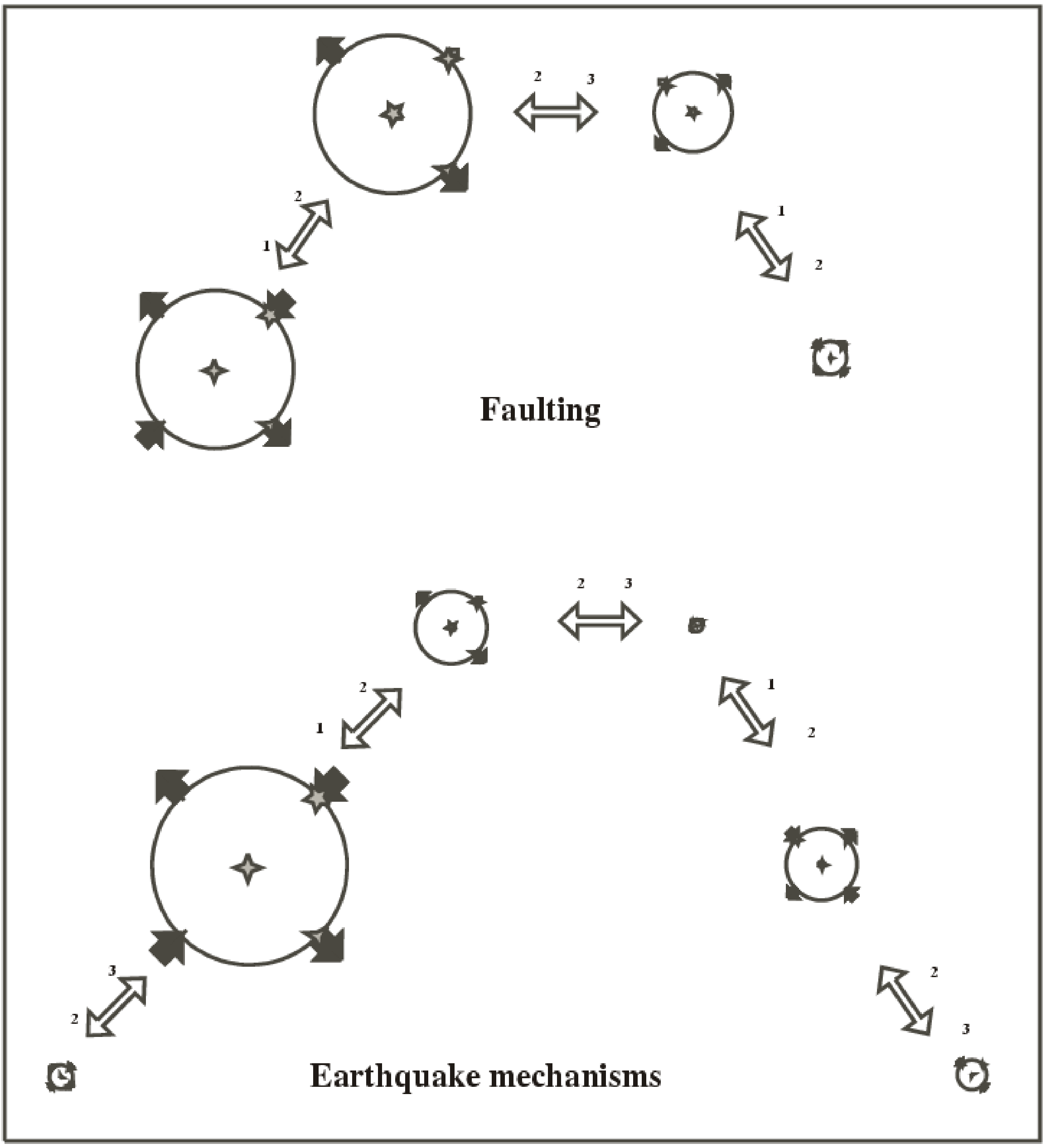

Figure 32. *The different stress tensors obtained from analyses of sets of fault-slip data and earthquake focal mechanisms in the SISZ (after Bergerat et al. 1999). Size of diagrams proportional to numbers of data. Three-, four-, and five-branched stars: regional axes of* σ_3, σ_2 *and* σ_1 *respectively (schematic). Couples of black arrows: directions of compression (convergent) or extension (divergent). Couples of open arrows: stress permutations (*σ_1/σ_2 *or* σ_2/σ_3 *modes) between the different regimes.*

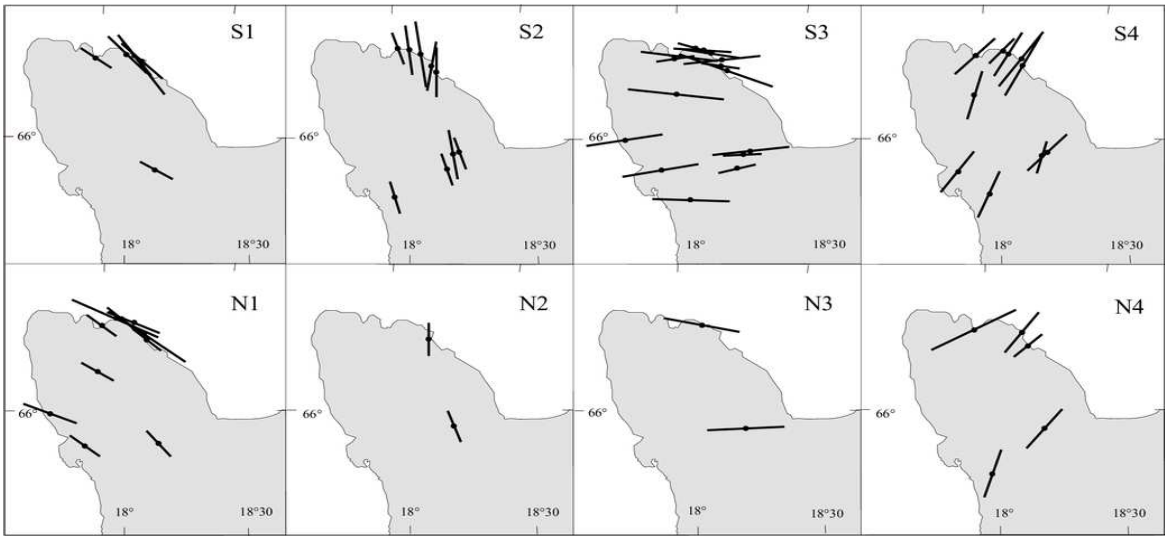

Figure 33. *Summary of local paleostress determinations made in Flateyjarskagi using Angelier's inversion (1990) (after Angelier et al. 2000b). Solid bars: trends of minimum compressive stress, σ_3. Bar size increases with quality of paleostress tensor determination. Nature of brittle tectonic regime: S-type for nearly vertical σ_2, N-type for nearly vertical σ_1.*

34). Such changes from very low mechanical coupling (weak fault) to moderate friction may occur very rapidly since it takes place several times in a few years, as shown by focal mechanisms of earthquakes analysis. Thus, the tectonic regimes need not be interpreted in terms of numerous tectonic episodes, but rather as a consequence of variable coupling across the transform zone.

3.6.2 Task 2: Reconstruction of the current stress field associated with the test areas

3.6.2.1 Task 2.1: Inversion of large sets of focal mechanisms of earthquakes

Using a new inversion technique suitable for focal mechanisms of earthquakes (in that it does not require the choice of a nodal plane as the actual fault plane) was particularly worthwhile in order to process the very large numbers of focal mechanisms of earthquakes determined within the SIL network set-up and monitored by IMOR.DG. This was because of the mathematical aspects which imply analytical resolution so that at the core of the inversion process itself the runtime does not depend on the quantity of data (Angelier 1998).

The inversion was carried out with a total dataset of about 50000 double–couple focal mechanisms of earthquakes (Angelier et al. 2000a). It revealed regional deviations as large as 40° in the direction of extension near the major transform zones (clockwise for the South Iceland seismic zone, counterclockwise for the Tjörnes fracture zone), relative to the N104°E trend of plate separation across the mid-Atlantic ridge. However, the mean axis of minimum stress obtained from these inversions for the whole of Iceland is quite consistent with the

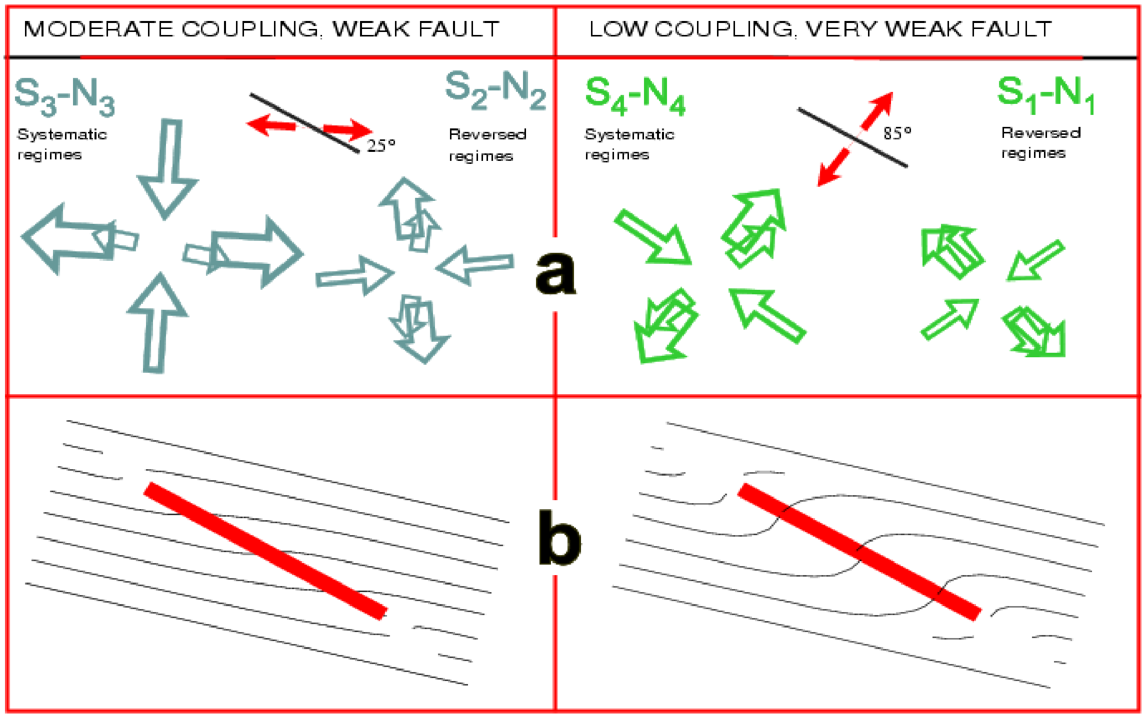

Figure 34. *Interpretation of tectonic regimes in terms of variable coupling near transform zone (after Angelier et al. 2000b). (a) Groups of tectonic regimes. Angles between transform direction (dotted lines) and averaged trends of extension (black arrows) indicated. (b) Schematic pattern of minimum compressive stress trajectories (thin lines) due to tensile loading parallel to spreading vector in North Iceland around oblique dextral transform fault zone (thick line).*

trend of plate separation independently reconstructed by DeMets et al. (1990).

3.6.2.2 Task 2.2: Seismotectonic analysis of individual faults

The Tjörnes fracture zone

The study of the Húsavík–Flatey fault in the Tjörnes fracture zone includes a tectonic analysis (see Subsection 3.6.1.2) and also a seismotectonic analysis in order to obtain a reconstruction of the stress patterns in accordance with the mechanisms of the transform zone since about 7 million years to the present (Garcia 1999; Garcia et al. 2000; Garcia et al., in preparation). We carried out an analysis of 669 double-couple earthquake mechanisms (period 1995-1997, magnitude ranging between 1 and 4.8). Three main sets of stress regimes have been identified, each including three individual stress regimes (Figure 35). The major one corresponds to an ENE-WSW trending right-lateral transtension. The two other regimes, less important, correspond to transform-parallel (WNW-ESE) and transform-perpendicular extensions (NNE-SSW).

Considering the angle between the trends of the rift and of the transform zone involves an extension occurring throughout the transform zone. This extension is accommodated by the transtensional regime, as well as, locally, by the extension sub-perpendicular to the transform direction. The extension sub-parallel to the transform direction may express by pull-apart process or by locking of part of the transform fault. The analysis of focal mechanisms of earthquakes indicates that most of these regimes currently occur, invalidating as well the hypothesis of polyphase tectonism (see Subsection 3.6.1.2). It suggests that transform motion along an oceanic fault zone may induce a variety of tectonic regimes. A major point of the transform mechanism is the variation of coupling along the HFF. These changes may correspond, at least partly, to the necessity of extension in this area because of the obliquity of the transform zone versus the rifts zones of N–Iceland and of Kolbeinsey, but the occurrence of magmatism at depth probably plays an important role also in such a phenomenon.

The Leirubakki fault

The Leirubakki fault is one of the large N-S seismic faults of the South Iceland seismic zone, located in its eastern part, a few kilometers west of the 1912 earthquake major earthquake. The Leirubakki rupture occurred earlier during historical times (maybe before the settlement of Iceland). Our work included the reconnaissance of the fault trace based on aerial photograph analysis and field study, a GPS mapping to reconstruct the morphology of the rupture zone, and some measurements of structures along the fault, including orientations and amplitudes (Bergerat et al. 2000; Bergerat et al., in preparation). We thus identify a pattern of dextral segments that connect typical push-up structures, with specific angular relationships between these features and the general trend of the earthquake fault (Figure 36). The fracturing process involved development of near-surface strike-slip segments, oblique relative to the underlying shear zone (Figure 36). We computed the shortening amounts and rock volumes involved in push-up development and estimated the magnitude of the Leirubakki fault to more than 7.

Figure 35. *Focal mechanisms of earthquakes characterizing the nine stress regimes in the Tjörnes fracture zone (SSR: strike-slip regime, NR: normal regime, RR: reverse regime) (after Garcia 1999; Garcia et al., in preparation). For the SSR2, SSR3, NR3 and RR4, only the focal mechanisms with M>1.8 are shown, for the other regimes all the focal mechanisms (M>1) are shown.*

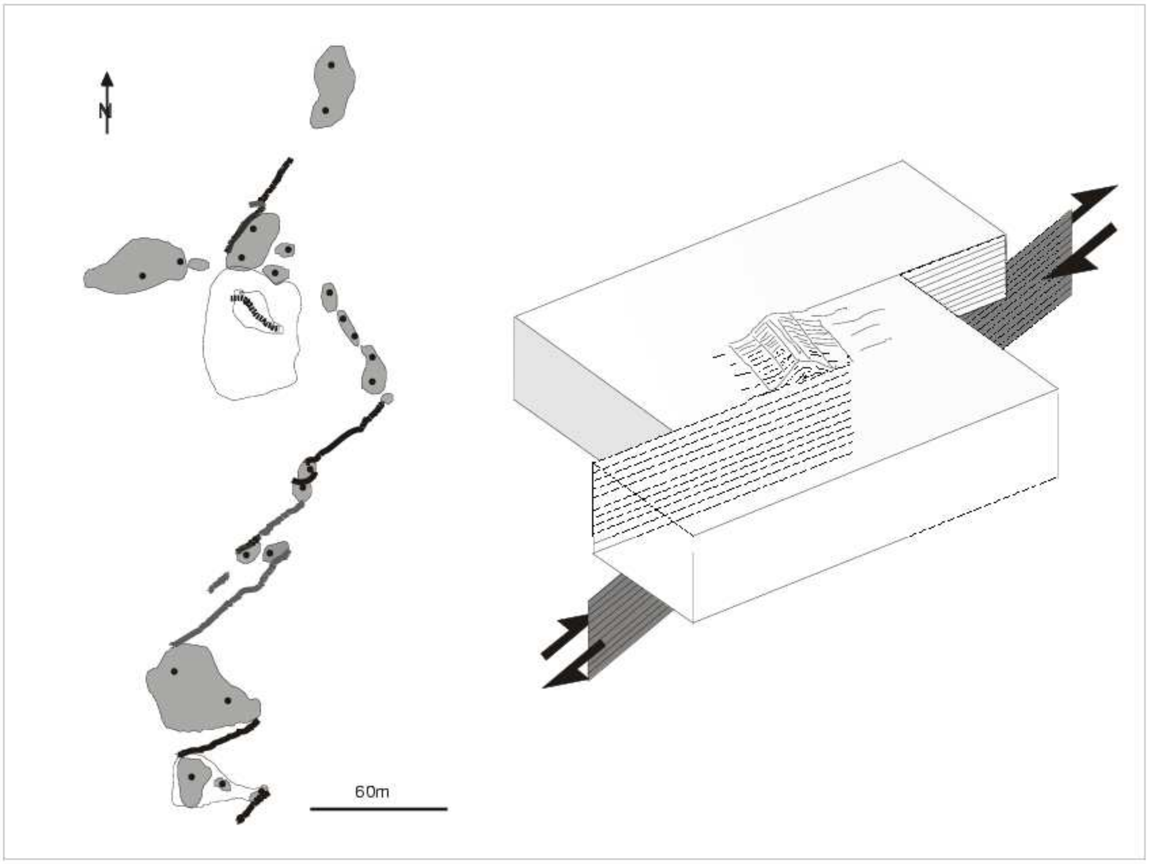

Figure 36. *The Leirubakki fault in the SISZ. On the left: detailed part of the map (drawn after GPS measurements) showing a typical array of individual fractures and individual push-ups. On the right: schematic view of a push-up and en-echelon fractures in the uppermost part of the crust and a single right-lateral strike-slip fault at depth (after Bergerat et al. 2000; Bergerat et al., in preparation).*

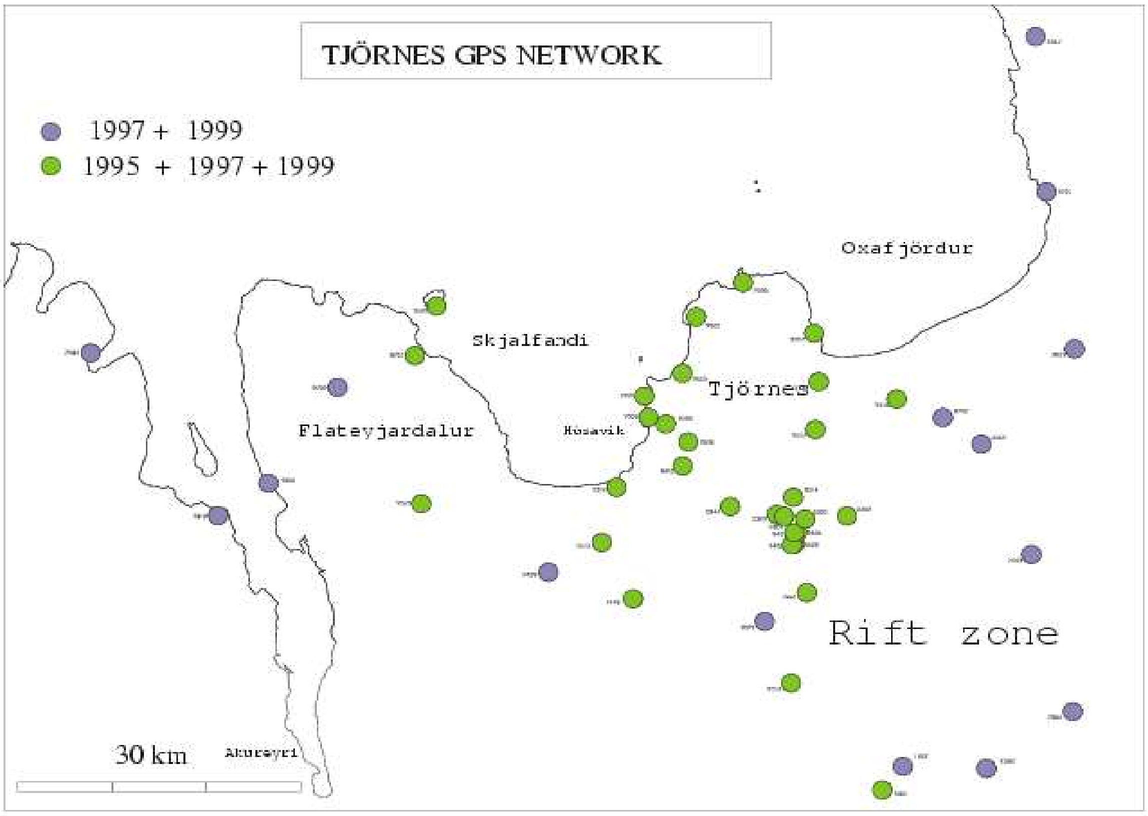

Figure 37. *The Tjörnes GPS network. 32 points have been measured in 1995, 1997 and 1999. The whole network has been measuring both in 1997 and 1999.*

3.6.3 Task 3: Present–day deformation from GPS network and interferograms of ERS-SAR scenes

3.6.3.1 Task 3.1: Measuring the present–day crustal displacements in the Tjörnes fracture zone and adjacent areas

The Tjörnes GPS network
The network consists of about 45 sites distributed in the northern Iceland seismic zone (Figure 37). It completes the geodetic networks already installed over the whole Iceland at a smaller scale. The TGN has been designed to measure the surface displacement field on each side of the Húsavík-Flatey fault (HFF). It has been done in order to estimate if there are locked fault segments in the area and how these segments can contribute to increase the seismic risk.

1995–1997 velocity field
The velocities (Figure 38) have been computed by reference to a point located in the southern part of the network. Two tendencies can be distinguished on the Tjörnes peninsula: eastward velocities reaching 13 mm/year for the most northern points of the peninsula and NNE velocities up to 15 mm/year for the points located on both sides of the HFF. Displacements